

Cellular Characterization of Microvascular Fragments and Stromal Vascular Fraction for the Treatment of Composite Bone-Muscle Defects

A Thesis
Presented to
The Academic Faculty

by

Yuyan Wang

In Partial Fulfillment
of the Requirements for the Degree
Bachelor of Science in the
School of Wallace H. Coulter Department of Biomedical Engineering

Georgia Institute of Technology
May 2017

Approved by:

Dr. Robert Guldberg, Advisor
George W. Woodruff School of Mechanical Engineering
Parker H. Petit Institute for Bioengineering and Bioscience
Georgia Institute of Technology

Dr. Nick Willett
Department of Orthopaedics
School of Medicine
Emory University

Date Approved: [Date Approved by Committee]

ACKNOWLEDGEMENTS

I wish to thank Marissa Ruehle, my graduate research mentor, for giving me the opportunity to work on this project. I would not have been where I am now if not for her kind support, both intellectually and emotionally, throughout my undergraduate years.

TABLE OF CONTENTS

	Page
ACKNOWLEDGEMENTS	2
SUMMARY	4
<u>CHAPTER</u>	
1 Introduction and Literature Review	5
2 Methods and Materials	8
2.1 MVF Isolation from adipose tissue	8
2.2 SVF Isolation from adipose tissue	8
2.3 Cell population identification	9
2.4 Cell preparation	10
2.7 Flow cytometry analysis	10
3 Results	12
4 Discussion	15
5 Conclusion	17
APPENDIX A: Cell preparation protocols	18
REFERENCES	21

SUMMARY

The current treatment for critical-sized bony defects, bone morphogenetic protein 2 (BMP-2) loaded collagen sponge grafting, is often inadequate for composite bone-muscle defects, which heal more slowly with higher rates of non- or malunion. Due to the additional muscle defect, there is a vacancy of vasculature around the bone defect, causing insufficient nutrient and cytokine delivery and thus hindering bone regeneration. Hypothesizing that increasing angiogenesis will improve regeneration, we have previously proposed to co-deliver microvascular fragments (MVF) or stromal vascular fraction (SVF), which have been shown to mature into microvascular networks *in vitro* and *in vivo*, with BMP-2 in a collagen sponge. However, in preliminary studies, collagen sponge co-loaded with BMP-2 and MVF showed augmented release of BMP-2 compared to those co-loaded with SVF or with BMP-2 only. Although they are both derived from the same adipose tissue source, we hypothesize that their cellular composition may differ and thus affect BMP-2 kinetics. Therefore, this project aims to characterize the cellular components of MVF and SVF using flow cytometry to elucidate the potential mechanism of differential BMP-2 release. It was found that MVF has a relatively lower percentage of mesenchymal stem cells (MSCs) and relatively higher percentage of mature endothelial cells (ECs) than SVF, suggesting a role for ECs in the augmented BMP-2 release from MVF-loaded collagen sponges.

CHAPTER 1

INTRODUCTION AND LITERATURE REIVEW

Bone can spontaneously heal and restore function and is one of the few organs in the body that does not undergo scarring¹. However, this mechanism is inadequate when dealing with critical sized bone defects. A critical sized bone defect is defined as an orthotopic defect that will not heal within the lifespan of the animal without intervention. Critical sized bone defects can arise from congenital defects, trauma, and tumor excision². Despite their prevalence and numerous clinically available approaches, effectively treating critical sized bone defects remains a challenge.

Bone grafting, surgical replacement of a missing bone segment with autogenic, allogenic or xenogenic material to restore its function, was the first treatment strategy utilized. Since the discovery of bone's osteoinductive capacity from its own demineralized, devitalized matrix in 1965, bioactive proteins, majorly cytokines, have been intensively researched for bone tissue regeneration purposes^{1, 3, 4}. Bone morphogenetic protein 2 (BMP-2), one of the most studied cytokines involved in bone regeneration, is a cytokine of the transforming growth factor beta (TGF- β) superfamily. It is naturally produced by osteoprogenitor cells, osteoblasts, and bone extracellular matrix (ECM) and is involved in promoting differentiation of osteoblasts from osteoprogenitor and mesenchymal cells⁵. Since the recent FDA approval, recombinant human bone morphogenetic protein 2 (rhBMP-2) loaded in collagen sponge has been utilized to treat critical sized bone defects^{6, 7}. Although this treatment has shown great efficacy compared to bone grafting alone, a high dosage of BMP-2 is required, and the mechanical performance of the regenerated bones do not match that of native bone tissue. Furthermore, high doses of BMP-2 can cause side effects such as cyst-like ectopic bone formation and soft tissue swelling⁸. Different BMP-2 delivery methods and grafting materials have been tested to achieve a better therapeutic outcome¹.

⁹. However, due to the lack of vascularization, the cells within large bone defects face inevitable death because of the lack of oxygen and other nutrients, thus hindering the clinical outcome of the BMP-2 treatment.

Muscle defects are almost always present along with critical sized bone defects. Not only does this affect the mechanical performance of the injured bone, but the missing vasculature resulting from the missing muscle also greatly hinders bone regeneration. It has been shown that even subtle reductions in bloodflow within the healing callus negatively influence the mechanical properties of the healing bone¹⁰. Thus, reconstructing an effective transportation system along with promoting osteogenesis is essential in treating critical sized bone defects. Current strategies of promoting vascularization include administering related growth factors, which are complicated by undesirable side effects and difficulties in cytokine delivery¹⁰. Other approaches involve implanting a pre-vascularized construct, where an initial vascular network is established in vitro by seeding a single cell type, or a combination of several cell types (mesenchymal stem cells, endothelial cells, etc.) into scaffolds for implantation into the injury site to promote the rapid reestablishment of vasculature¹¹⁻¹³. Microvascular fragments (MVF) are a multicellular vascular construct obtained from adipose tissue. Stromal vascular fraction (SVF) is a single cell level population that consists of multiple cell types, including endothelial, muscle, stem and other cell types, that is also obtained from adipose tissue. It has been shown that MVF can elongate in collagen gel in vitro, and transplanted MVF can rapidly develop into blood-perfused networks in vivo^{14, 15}. Rather than seeding a single cell type, seeding MVF or SVF can potentially be more efficient, as they tend to inosculate more quickly and form more mature vessels. Both MVF and SVF can be isolated from adipose tissue, thus enabling autologous use. Additionally, MVFs and

SVFs may be rich sources of mesenchymal stem cells, which makes them promising candidates in the context of bone regeneration¹⁵.

We propose to use a BMP-2 loaded collagen sponged seeded with MVF or SVF (*figure 1*) as a more effective strategy for treating critical-sized bone-muscle composite defects. The BMP-2 serves to promote osteogenesis, while MVF and SVF further enhance the therapeutic effect by providing the vasculature critical to bone regeneration. Previous research done toward this project revealed a difference in the BMP-2 release profile of BMP-2 loaded collagen sponges seeded with MVF and SVF. BMP-2 loaded collagen sponges seeded with MVF showed a greater release of BMP-2 than those of acellular or SVF seeded sponges. We aim to uncover the cause of this different BMP-2 release profile, which may augment our treatment strategy, by characterizing the cellular components of SVF and MVF using flow cytometry.

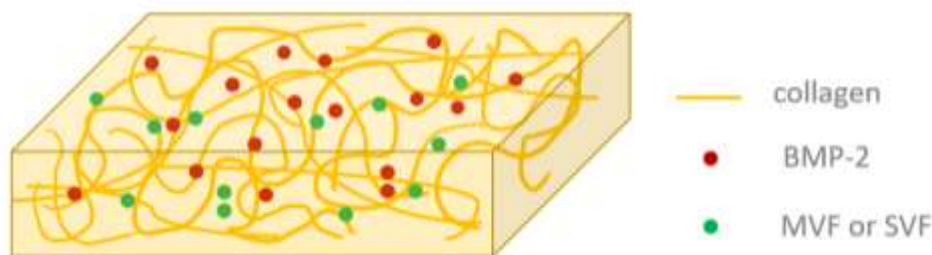


Figure 1 Schematics of BMP-2 and MVF/SVF loaded collagen sponge (not to scale)

It was hypothesized that mesenchymal stem cells (MSC), pericytes, mature endothelial cells (EC), EC progenitors, and smooth muscle cells (SMC) are present in both MVF and SVF but that their relative proportions may differ, thus enabling different cellular interactions with BMP-2 between the two groups. More specifically, a higher proportion of MSCs present in MVF was hypothesized to be the main cause of this increased BMP-2 release through MSC-BMP-2 interactions.

CHAPTER 2

METHODS AND MATERIALS

2.1 MVF isolation from adipose tissue

Epididymal fats were harvested from male retired breeder rats under isoflurane induced anesthesia. The fat was placed in a tube with HBSS with 5% FBS. Fat pads were manually minced for 7-8 minutes until a homogenous mixture was obtained. Minced adipose tissue was then chemically digested (per mL fat: 1.5 mL PBS (Sigma Aldrich), 0.75 g BSA (Sigma Aldrich), 2 mg DNase (Sigma Aldrich), 3.5 mg collagenase (Worthington)) with agitation at 37 °C. Digestion was stopped by adding serum-containing HBSS at a minimum 1:1 volumetric ratio. The digested solution was then centrifuged at 4000 rpm for 4 minutes in 50 mL conical tubes to allow removal of fat globules. The vascular pellet was then washed and resuspended in FBS-HBSS and centrifuged at 3000 rpm for 3 minutes in 15 mL conical tubes twice. Pellets were re-suspended in BSA-PBS and filtered first through a 200 µm nylon filter to remove residual large tissue pieces, then through a 20 µm filter membrane to remove single cells. MVF were collected by washing the 20 µm membrane with 40 – 50mL FBS-HBSS solutions (*Figure 2*)¹⁴.

2.2 SVF isolation from adipose tissue

The procedure for SVF isolation is similar to that of MVF, but the chemical digestion was done on a shaker at 225 rpm at 37°C for 30 minutes in order to break down the vascular components to the single cell level. SVF was filtered in the same manner as MVF; however, the flow-through passing the 20µm filter was collected as single cell SVF.

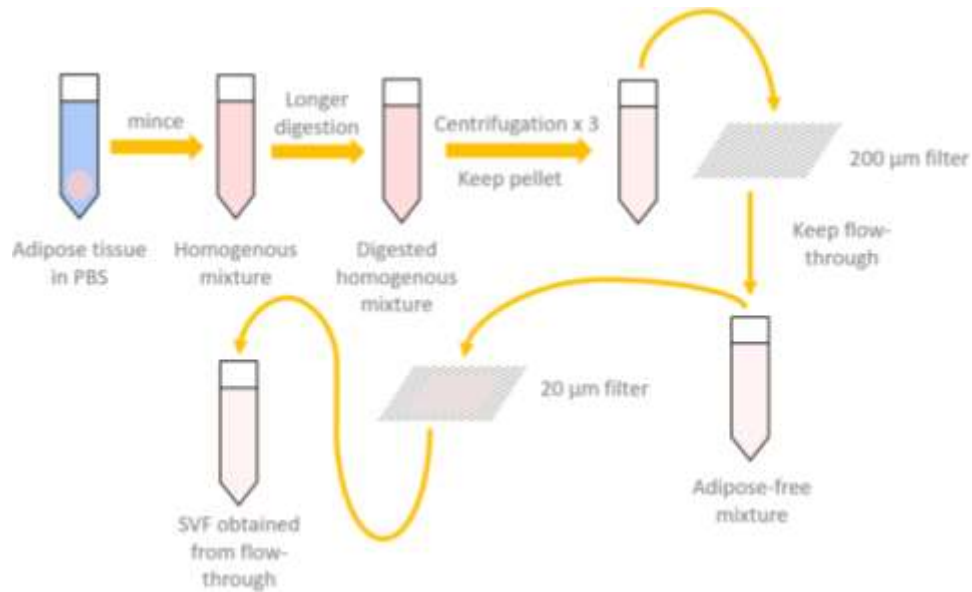


Figure 2. Schematic of SVF isolation

2.3 Panel selection

The cell populations of interest are MSCs, pericytes, mature and progenitor ECs, and SMCs. While red blood cells (RBC) are present, they were not examined in this study; thus, they were eliminated during cell preparation. A panel of MSC markers (CD29+CD90+CD45-) was selected from MSC markers commonly used in previously published literature¹⁶⁻¹⁸. Both pericytes and SMCs express alpha smooth muscle actin (ASMA), but NG2 expression is exclusive to pericytes. CD31 is a common marker for EC and is shared by pericytes. EC progenitors also express CD34; however, as EC mature, CD34 expression is lost¹⁸. Thus, the remaining four populations were classified as pericytes (ASMA+NG2+CD31+), SMCs (ASMA+NG2-CD31-CD34-), mature ECs (ASMA-NG2-CD31+CD34-), and EC progenitors (ASMA-NG2-CD31+CD34-).

The seven markers chosen were divided into two panels to be prepared and analyzed separately in order to minimize the spectral overlap between the channels. MSCs were identified in panel 1, while both mature and progenitor endothelial cells, pericytes, and smooth muscle cells were identified in panel 2. All antibodies used were fluorochrome conjugated, and the

combinations of fluorochromes in each panel were selected with the assistance of Fluorescence Spectrum Viewer from BD Bioscience to ensure minimal spectral overlap. Table 2 summarizes the antibodies used in each panel^{19, 20}.

Table 1. Cell population classifications for pericytes, EC (mature and progenitor) and SMC.

	Pericytes	EC (mature)	EC (progenitor)	SMC
ASMA	+	-	-	+
NG2	+	-	-	-
CD31	-	+	+	-
CD34	/	-	+	-

2.4 Cell preparation

After MVF and SVF collection, the cells were incubated in 6 mL of 1X RBC lysis buffer for 5 minutes to remove red blood cells. The cells were then divided into single stain control, fluorescence minus one (FMO) control, and experimental groups. Detailed staining protocols for both panels are listed in Appendix A. The samples were analyzed by flow cytometry immediately after the staining was completed.

Table 2. Antibodies used in each panel

Target	Fluorochrome	Manufacture	Catalog number
Panel 1			
CD29	PE/Cy7	BioLegend	102222
CD45	PE	BioLegend	202207
CD90	Alexa Fluor 488	BioLegend	202506
Panel 2			
NG2	Alexa Fluor 350	Bioss	bs-5829R-A350
ASMA	FITC	abcam	ab8211
CD34	PE	abcam	ab187284
CD31	Alexa Fluor 647	Bio-Rad	MCA1334A647

2.5 Flow cytometry analysis

Samples were analyzed on BD FACS Aria™ Fusion with a 100µm nozzle immediately following staining. Data was analyzed on FlowJo V10). Each panel of MVF and SVF were collected and analyzed separately following the same protocols. Voltage optimizations were conducted before every analysis, and compensations were calculated based on freshly made single stained control groups. Positive and negative gating thresholds for each channel were determined by the FMO controls (*Figure 3*).

For both panels, debris and doublets were excluded by gating on area of forward scatter (FSC-A) vs. area of side scatter (SSC-A) and FSC-A vs. height of forward scatter (FSC-H). For panel 1, the CD29+CD90+ population was gated, from which the MSC (CD29+CD90+CD45-) population was identified. For panel 2, The ASMA+NG2- and ASMA+NG2+ populations were first gated, and from each population, a CD34 vs. CD31 plot was created. From the ASMA+NG2- population, the SMC (ASMA+NG2-CD31-CD34-), mature EC (ASMA-NG2-CD31+CD34-), and EC progenitor (ASMA-NG2-CD31+CD34-) populations were identified; from the ASMA+NG2+ populations, the pericyte (ASMA+NG2+CD31+) population was identified.

CHAPTER 3

RESULTS

From the FMO controls, the gating thresholds were determined (Figure 3). For SVF panel 1, Alexa Fluor 488 positive was above 3×10^3 , PE/Cy7 positive was above 2×10^3 , and PE positive was above 1×10^4 ; for MVF panel 1, Alexa Fluor 488 positive was above 1×10^4 , PE/Cy7 positive was above 1×10^3 , and PE positive was above 1×10^4 . For SVF panel 2, FITC positive was above 3×10^2 , PE positive was above 3×10^2 , Alexa Fluor 647 positive was above 3×10^2 , and Alexa Fluor 350 was above 2×10^3 ; for MVF panel 2, FITC positive was above 1×10^4 , PE positive was above 1×10^4 , Alexa Fluor 647 positive was above 1×10^3 , and Alexa Fluor 350 was above 1×10^4 .

SVF contains a higher percentage of MSC (CD29+CD90+CD45-) than MVF, with SVF containing 18.38% MSCs and MVF containing 10.79% MSCs. *Figure 4* shows the gating sequence. Additionally, SVF has higher percentages of SMC (ASMA+NG2-CD31-CD34-) (37.04%) and pericytes (ASMA+NG2+CD31+) (6.59%) than MVF (0.35% and 0.63%, respectively). In contrast, mature EC (ASMA-NG2-CD31+CD34-) comprise a higher proportion of MVF (23.72%) than SVF (3.15%). Both SVF and MVF have very low content of endothelial cell progenitors (ASMA+NG2-CD31+CD34+) (0.17% and 0.12%, respectively).

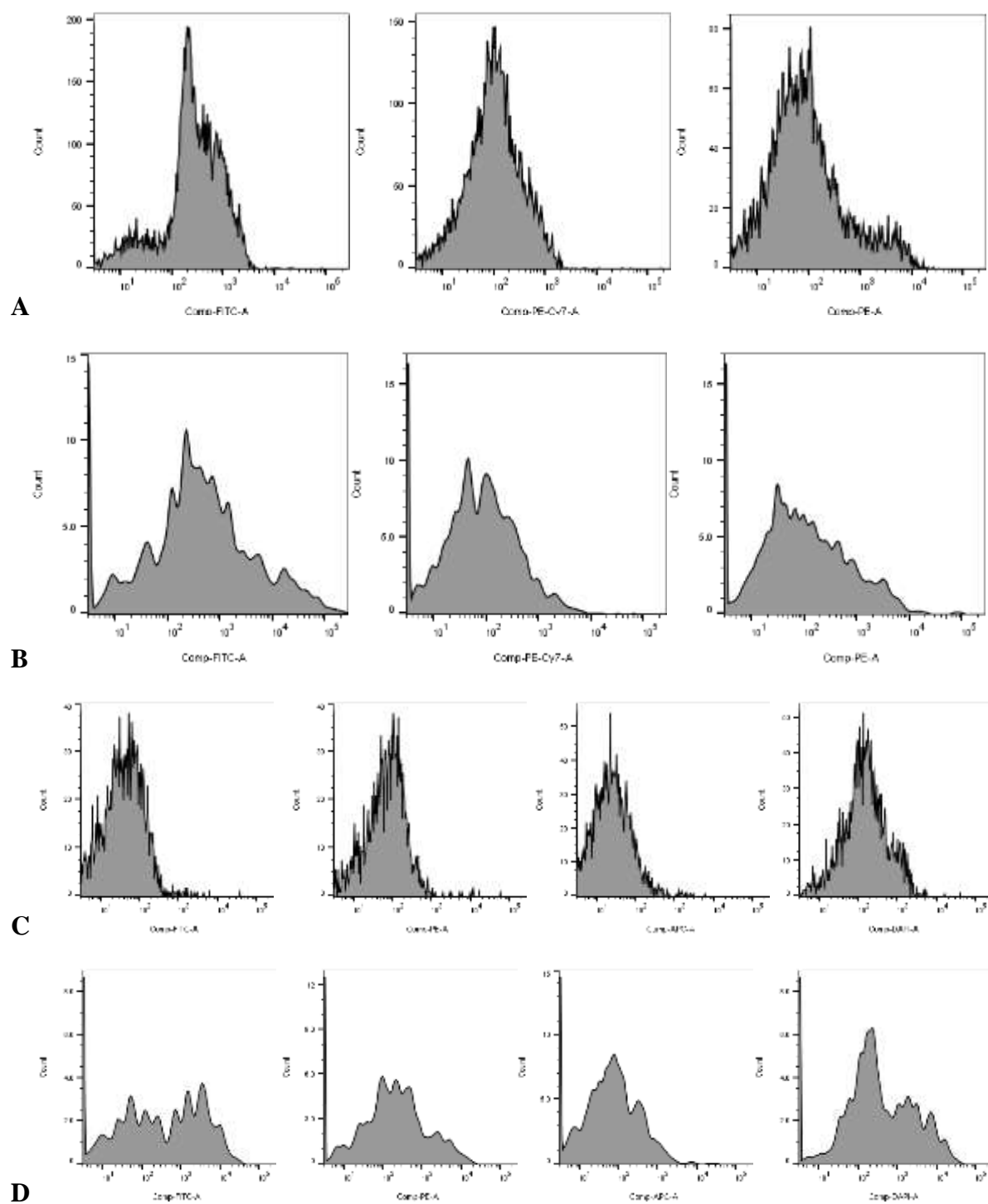


Figure 3. FMO control of a) SVF panel 1, b) MVF panel 2, c) SVF panel 2, and d) MVF panel 2.

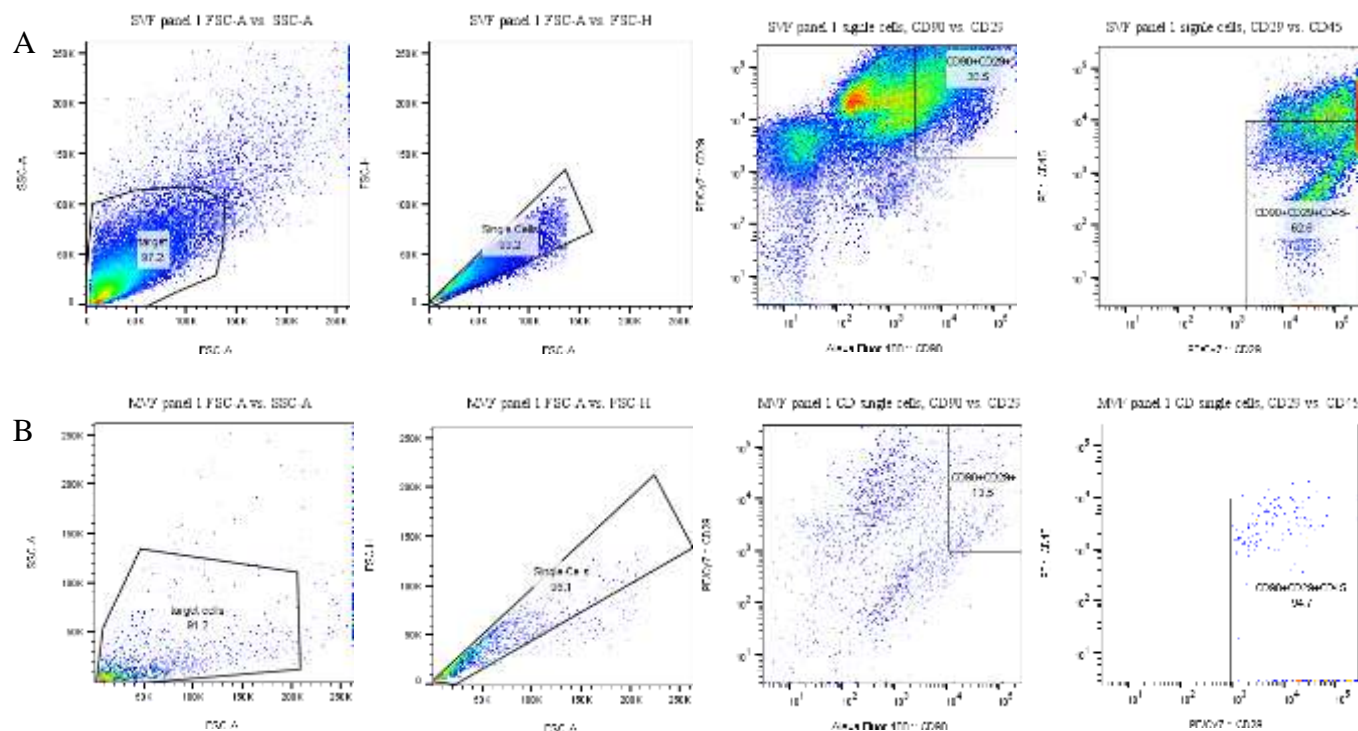


Figure 4. gating sequences of a) SVF and b) MVF panel 1. In SVF, CD29+CD90+CD45- MSC: 18.38%. In MVF, CD29+CD90+CD45- MSC: 10.79%.

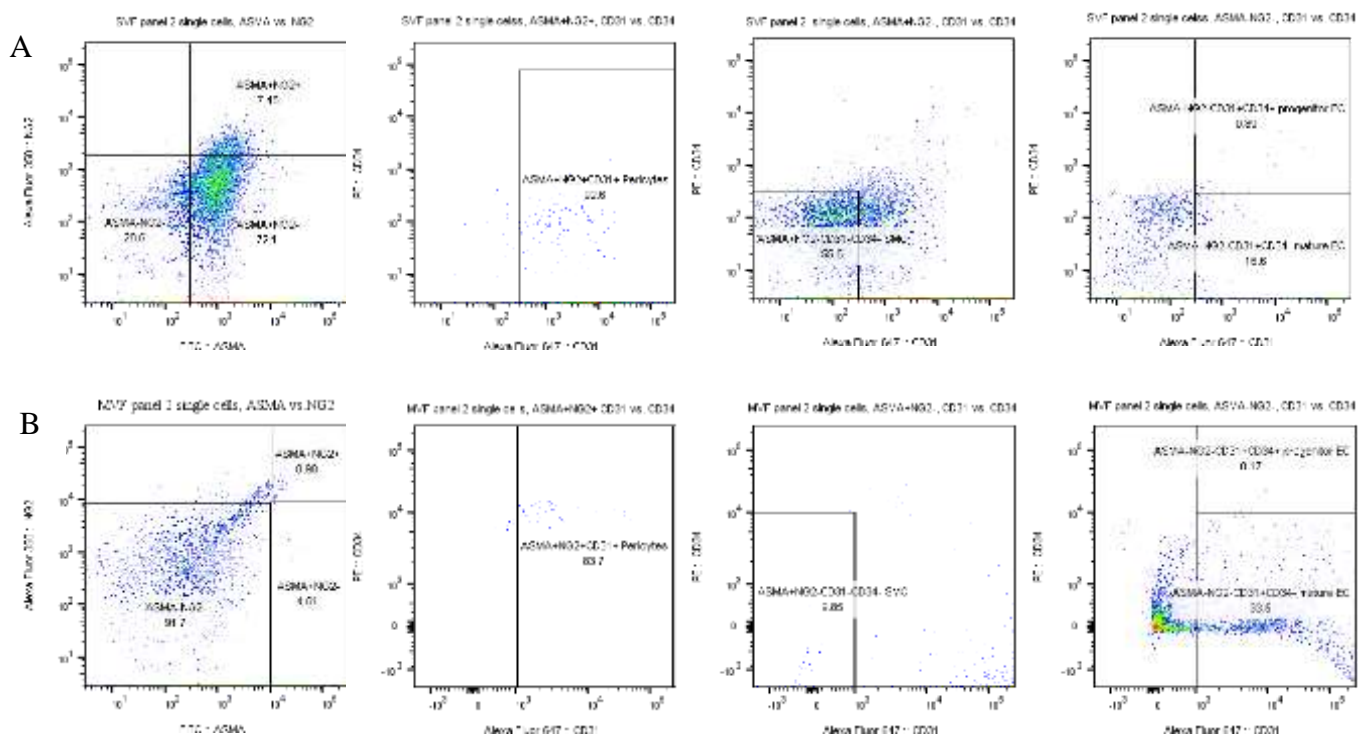


Figure 5. gating sequences of a) SVF and b) MVF panel 2. In SVF, ASMA+NG2-CD31-CD34- SMC: 37.04%; ASMA+NG2+CD31+ pericytes: 6.39%; ASMA-NG2-CD31+CD34- mature EC: 3.15%; ASMA-NG2-CD31+CD34+ progenitor EC: 0.17%. In MVF, ASMA+NG2-CD31-CD34- SMC: 0.35%; ASMA+NG2+CD31+ pericytes: 0.63%; ASMA-NG2-CD31+CD34- mature EC: 23.72%; ASMA-NG2-CD31+CD34+ progenitor EC: 0.12%.

CHAPTER 4

DISCUSSION

It was hypothesized that the difference in the BMP-2 release profiles was due to different cellular components of MVF and SVF, and one possible cause of greater BMP-2 release in MVF was a higher proportion of MSCs. However, it was observed in this study that SVF has a higher percentage of MSC than MVF. Hence, MSC-released BMP-2 causing the difference between the SVF and MVF BMP-2 release curves is unlikely. During BMP-2 signaling, BMP-2 receptors are internalized upon binding to the ligand, and it has been observed in a study done by Alborzinia *et.al.* that the BMP-2 ligands were also increasingly internalized to the cell center in a time-dependent manner²¹. Thus, it is possible that the greater BMP-2 release in the MVF group was not due to the endogenously secreted BMP-2 by MSCs but rather to feedback mechanisms of greater BMP-2 uptake in SVF. However, this does not explain the BMP-2 release profile in the acellular group being less than that of the MVF group. Other than the differences in MSC populations, SMC, pericyte and mature EC populations are also distinctively different in SVF and MVF. It is possible that the BMP-2 release profile is related to the BMP-2 EC interactions. Bouletreau *et. al.* showed in 2002 that upon stimulation with vascular endothelial growth factor (VEGF), BMP-2 mRNA in EC was upregulated²². Additionally, other studies demonstrated upregulation of BMP-2 gene expression in vascular EC or upregulation of BMP-2 receptors in cells co-cultured with EC under various conditions²³⁻²⁵. VEGF is a key driver of angiogenesis and is expressed by MVF and SVF²⁶. It was observed in this study that a higher percentage of mature EC is present in MVF than in SVF, which could possibly explain the greater release of BMP-2 in the MVF group.

A limitation of this study is that adipose-derived cells have significant autofluorescence when excited by shorter wavelengths (violet or blue)²⁷. Due to restrictions on minimizing spectrum

overlaps, some fluorochromes that are excited at shorter wavelength (such as Alexa Fluor 350, Alexa Fluor 488/FITC) were included in our panels. This may have affected the collection of the data; some true positive signals may not be detected due to high autofluorescence at the same wavelength, rendering an inaccurate population profile.

CHAPTER 5

CONCLUSION

It was originally hypothesized that a higher percentage of MSCs present in MVF than SVF caused the greater BMP-2 release profile of MVF-loaded collagen sponges compared to acellular or SVF-loaded sponges. This study did not support that hypothesis; however, it demonstrated that the SVF and MVF differ in their cellular profiles. The percentage of ECs is much higher in MVF (23.72%) compared to SVF (3.15%). This may be the cause of the greater BMP-2 release, as prior studies have demonstrated that ECs are capable of producing BMP-2. However, further studies are needed to confirm this hypothesis. Future work may include co-loading collagen sponge with fluorescently labeled BMP-2 and MVF or SVF to determine whether the excess BMP-2 present in the MVF group is released exogenous growth factor or produced (non-labeled) BMP-2. Alternatively, BMP-2 mRNA expression in MVF and SVF can be examined, or ECs can be transfected to express labeled BMP-2 to investigate the source of the excess BMP-2.

APPENDIX A

CELL PREPARATION PROTOCOLS

Obtain MVF and SVF as described in section 2.1 and 2.2. Digest MVF further down to single cell level in 3 mL digestion solution on a shaker at 225 rpm at 37 C for 30 minutes. Incubate both SVF and MVF in 6mL of 1X RBC lysis buffer for 5 minutes at room temperature. Centrifuge at 1,500 rpm for 5 minutes, discard supernatant, and resuspend in 2 mL of 10% FBS in 1X PBS (staining buffer). Centrifuge again at 1,500 for 5 minutes and perform cell counting. The final cell concentration should be around 1-2 million cells per milliliter.

eBioscience OneComp Beads are used for negative makers, such as CD45 and CD34.

A.1 Cell preparation for panel 1

1. Aliquot the cell suspension into 7 1.5 mL Eppendorf tubes with 200 μ L in each;
2. Add 60 μ L of OneComp beads, 138 μ L of staining buffer and 2 μ L of anti-CD45-PE antibody into a separate 1.5 mL Eppendorf tube;
3. Add appropriate antibody to the 8 tubes as indicated in the table below (use beads for PE single stain control as indicated in step 2)

	<i>Unstained</i>	<i>Single stain controls</i>			<i>FMO controls</i>			<i>Experimental</i>
<i>Anti-CD29-PE/Cy7</i>	-	2 μ L	-	-	-	2 μ L	2 μ L	2 μ L
<i>Anti-CD45-PE</i>	-	-	2 μ L*	-	2 μ L	-	2 μ L	2 μ L
<i>Anti-CD90-Alexa Fluor 488</i>	-	-	-	2 μ L	2 μ L	2 μ L	-	2 μ L

Table 3. Panel 1 cell preparation

*using OneComp beads instead of cells

4. Incubate at room temperature for 30 minutes, protected from light;
5. Centrifuge at 300 x g for 5 minutes, discard supernatant and resuspend in 200 μ L of staining buffer;

6. Centrifuge again at 300 x g for 5 minutes, discard supernatant and resuspend in 400 μ L of staining buffer;

7. Transfer to flow tube, analyze immediately. One can resuspend the cells in staining buffer containing 1% sodium azide during the last step to allow more time between staining and analysis. However, the samples should be analyzed within the same day to ensure optimal results. If same day analysis is not possible, sample should be fixed in 100 μ L 1% PFA in PBS at 4-degree C for 10 minutes. Resuspend in staining buffer. The samples can then be stored in 4-degree fridge for up to one week.

A.2 Cell preparation for panel 2

1. Aliquot the cell suspension into 9 1.5 mL Eppendorf tubes with 200 μ L in each;
2. Add 60 μ L of OneComp beads, 138 μ L of staining buffer and 2 μ L of anti-CD34-PE antibody into a separate 1.5 mL Eppendorf tube;
3. Add appropriate antibody to the 10 tubes as indicated in the table below (use beads for PE single stain control as indicated in step 2). NOTE: although it is listed in the table, no anti-ASMA-FITC antibody should be added at this point.

	<i>Unstained</i>	<i>Single stain controls</i>				<i>FMO controls</i>				<i>Experimental</i>
<i>TUBE#</i>	1	2	3*	4	5	6	7	8	9	10
<i>Anti-ASMA-FITC</i>	-	2 μ L	-	-	-	-	2 μ L	2 μ L	2 μ L	2 μ L
<i>Anti-CD34-PE</i>	-	-	2 μ L	-	-	2 μ L	-	2 μ L	2 μ L	2 μ L
<i>Anti-CD31-Alexa Fluor 647</i>	-	-	-	2 μ L	-	2 μ L	2 μ L	-	2 μ L	2 μ L
<i>Anti-NG2-Alexa Fluor 350</i>	-	-	-	-	2 μ L	2 μ L	2 μ L	2 μ L	-	2 μ L

Table 4. panel 2 cell preparation

*using OneComp beads instead of cells

4. Incubate at room temperature for 30 minutes, protected from light;
5. Centrifuge at 300 x g for 5 minutes, discard supernatant and resuspend in 200 μ L of staining buffer;

6. Centrifuge again at 300 x g for 5 minutes, discard supernatant and resuspend in 100 μ L of 1% PFA in PBS;
7. Incubated at 4-degree C for 10 minutes;
8. Centrifuge at 300 x g for 5 minutes, discard supernatant and
 - a. Resuspend tubes 2,7,8,9, and 10 in 100 μ L of 0.5% Tween 20 in PBS;
 - b. Resuspend tubes 1,3,4,5, and 6 in 100 μ L of staining buffer;
9. Incubate at room temperature for 20 minutes;
10. Centrifuge all tubes at 300 x g for 5 minutes, discard supernatant and
 - a. Resuspend tubes 2,7,8,9, and 10 in 200 μ L of staining buffer;
 - b. Resuspend tubes 1,3,4,5, and 6 in 400 μ L of staining buffer, transfer to flow tubes;
11. Add 2 μ L of anti-ASMA-FITC antibody into tubes 2,7,8,9, and 10, incubated at room temperature for 30 minutes;
12. Centrifuge at 300 x g for 5 minutes, discard supernatant and resuspend in 200 μ L of staining buffer;
13. Centrifuge at 300 x g for 5 minutes, discard supernatant and resuspend in 400 μ L of staining buffer;
14. Transfer to flow tubes, analyze within one week.

REFERENCES

1. Egermann, M. *et al.* Effect of BMP-2 gene transfer on bone healing in sheep. *Gene Ther* **13**, 1290-1299 (2006).
2. Spicer, P.P. *et al.* Evaluation of bone regeneration using the rat critical size calvarial defect. *Nat. Protocols* **7**, 1918-1929 (2012).
3. Kempen, D.H.R. *et al.* Retention of in vitro and in vivo BMP-2 bioactivities in sustained delivery vehicles for bone tissue engineering. *Biomaterials* **29**, 3245-3252 (2008).
4. Urist, M.R. Bone: formation by autoinduction. *Science (New York, N.Y.)* **150**, 893-899 (1965).
5. Lieberman, J.R., Daluiski, A. & Einhorn, T.A. The role of growth factors in the repair of bone. Biology and clinical applications. *The Journal of bone and joint surgery. American volume* **84-a**, 1032-1044 (2002).
6. Kolambkar, Y.M. *et al.* Spatiotemporal delivery of bone morphogenetic protein enhances functional repair of segmental bone defects. *Bone* **49**, 485-492 (2011).
7. Willett, N.J. *et al.* Attenuated human bone morphogenetic protein-2-mediated bone regeneration in a rat model of composite bone and muscle injury. *Tissue engineering. Part C, Methods* **19**, 316-325 (2013).
8. Zara, J.N. *et al.* High Doses of Bone Morphogenetic Protein 2 Induce Structurally Abnormal Bone and Inflammation In Vivo. *Tissue Engineering. Part A* **17**, 1389-1399 (2011).
9. Kolambkar, Y.M. *et al.* An Alginate-based Hybrid System for Growth Factor Delivery in the Functional Repair of Large Bone Defects. *Biomaterials* **32**, 65-74 (2011).
10. Krishnan, L., Willett, N.J. & Guldberg, R.E. Vascularization Strategies for Bone Regeneration. *Annals of Biomedical Engineering* **42**, 432-444 (2014).
11. Brennan, M.A., Davaine, J.-M. & Layrolle, P. Pre-vascularization of bone tissue-engineered constructs. *Stem Cell Research & Therapy* **4**, 96-96 (2013).
12. Kaempfen, A. *et al.* Engraftment of Prevascularized, Tissue Engineered Constructs in a Novel Rabbit Segmental Bone Defect Model. *International Journal of Molecular Sciences* **16**, 12616-12630 (2015).
13. Pedersen, T.O. *et al.* Endothelial microvascular networks affect gene-expression profiles and osteogenic potential of tissue-engineered constructs. *Stem Cell Research & Therapy* **4**, 52-52 (2013).
14. Hoying, J.B., Boswell, C.A. & Williams, S.K. Angiogenic potential of microvessel fragments established in three-dimensional collagen gels. *In Vitro Cellular & Developmental Biology - Animal* **32**, 409-419 (1996).
15. Laschke, M.W. & Menger, M.D. Adipose tissue-derived microvascular fragments: natural vascularization units for regenerative medicine. *Trends in Biotechnology* **33**, 442-448.
16. BÜHring, H.-J. *et al.* Novel Markers for the Prospective Isolation of Human MSC. *Annals of the New York Academy of Sciences* **1106**, 262-271 (2007).
17. Lv, F.-J., Tuan, R.S., Cheung, K.M.C. & Leung, V.Y.L. Concise Review: The Surface Markers and Identity of Human Mesenchymal Stem Cells. *STEM CELLS* **32**, 1408-1419 (2014).

18. Zimmerlin, L. *et al.* Stromal vascular progenitors in adult human adipose tissue. *Cytometry. Part A : the journal of the International Society for Analytical Cytology* **77**, 22-30 (2010).
19. , Vol. 2017 (BD Biosciences, 2017).
20. Church, C., Berry, R. & Rodeheffer, M.S. Isolation and Study of Adipocyte Precursors. *Methods in enzymology* **537**, 31-46 (2014).
21. Alborzinia, H. *et al.* Quantitative kinetics analysis of BMP2 uptake into cells and its modulation by BMP antagonists. *Journal of Cell Science* **126**, 117 (2013).
22. Bouletreau, P.J. *et al.* Hypoxia and VEGF up-regulate BMP-2 mRNA and protein expression in microvascular endothelial cells: implications for fracture healing. *Plastic and reconstructive surgery* **109**, 2384-2397 (2002).
23. Basic-Jukic, N. *et al.* Expression of BMP-2 in Vascular Endothelial Cells of Recipient May Predict Delayed Graft Function After Renal Transplantation. *Kidney & blood pressure research* **41**, 781-793 (2016).
24. Li, R., Nauth, A., Gandhi, R., Syed, K. & Schemitsch, E.H. BMP-2 mRNA expression after endothelial progenitor cell therapy for fracture healing. *Journal of orthopaedic trauma* **28 Suppl 1**, S24-27 (2014).
25. Talavera-Adame, D. *et al.* Bone morphogenetic protein-2/-4 upregulation promoted by endothelial cells in coculture enhances mouse embryoid body differentiation. *Stem cells and development* **22**, 3252-3260 (2013).
26. Krishnan, L., Hoying, J.B., Nguyen, H., Song, H. & Weiss, J.A. Interaction of angiogenic microvessels with the extracellular matrix. *American journal of physiology. Heart and circulatory physiology* **293**, H3650-3658 (2007).
27. Cho, K.W., Morris, D.L. & Lumeng, C.N. Flow Cytometry Analyses of Adipose Tissue Macrophages. *Methods in enzymology* **537**, 297-314 (2014).